Biomicrofluidics ARTICLE scitation.org/journal/bmf

# A liver-on-a-chip for hepatoprotective activity assessment

Cite as: Biomicrofluidics 14, 064107 (2020); doi: 10.1063/5.0024767
Submitted: 11 August 2020 · Accepted: 14 November 2020 ·
Published Online: 30 November 2020



Jiu Deng,[1,2] Ye Cong,[1] Xiahe Han,[3] Wenbo Wei,[4] Yao Lu,[2] Tingjiao Liu,[5] Weijie Zhao,[1] Bingcheng Lin,[2] Yong Luo,[1,a)] and Xiuli Zhang[3,a)]

## AFFILIATIONS

[1]State Key Laboratory of Fine Chemicals, Department of Pharmaceutical Sciences, School of Chemical Engineering, Dalian University of Technology, 116024 Dalian, China
[2]Biotechnologhy Division, Dalian Institute of Chemical Physics, Chinese Academy of Sciences, 116023 Dalian, China
[3]College of Pharmaceutical Science, Soochow University, 215123 Suzhou, China
[4]Shenzhen Institute of Geriatrics & Shenzhen Second People's Hospital, First Affiliated Hospital of Shenzhen University, 518000 Shenzhen, China
[5]College of Stomatology, Dalian Medical University, 116044 Dalian, China

[a)]**Authors to whom correspondence should be addressed:** zhangxl@suda.edu.cn and yluo@dlut.edu.cn

## ABSTRACT

Hepatoprotectant is critical for the treatment of liver disease. This study first reported the application of a liver chip in the hepatoprotective effect assessment. We first established a biomimetic sinusoid-on-a-chip by laminating four types of hepatic cell lines (HepG2, HUVEC, LX-2, and U937 cells) in a single microchannel with the help of laminar flow in the microchannel and some micro-fences. This chip was straightforward to fabricate and operate and was able to be long-term cultured. It also demonstrated better hepatic activity (cell viability, albumin synthesis, urea secretion, and cytochrome P450 enzyme activities) over the traditional planar cell culture model. Then, we loaded three hepatoprotectants (tiopronin, bifendatatum, and glycyrrhizinate) into the chip followed by the addition of acetaminophen as a toxin. We successfully observed the hepatoprotective effect of these hepatoprotectants in the chip, and we also found that bifendatatum predominantly reduced alanine transaminase secretion, tiopronin predominantly reduced lactate dehydrogenase secretion, and glycyrrhizinate predominantly reduced aspartate transaminase secretion, which revealed the different mechanisms of these hepatoprotectants and provided a clue for following molecular biological study of the protecting mechanism.



## INTRODUCTION

Liver diseases such as viral hepatitis, alcoholic liver disease, drug-induced liver injury, cirrhosis, and non-alcoholic steatohepatitis endanger human life and health[1] by jeopardizing the metabolism, digestion, detoxification, and immunity of the human body.[2] Liver disease therapy thus is important for patients, in which hepatoprotective drugs play critical roles.

Animal testing usually is widely used for developing hepatoprotective drugs; however, it is expensive, time consuming, and sometimes misleading due to cross-species difference.[3] *In vitro* cell models generally are fast and are operated in a high throughput manner, but they cannot reflect the complex physiological functions of human tissues and organs due to lacking physiologically relevant arrangement, cellular communication, appropriate shear force, etc.[4,5]

Organ-on-a-chip is a cutting-edge technology able to reconstruct the key features of specific human tissues and organs (such as liver,[6,7] kidney,[8,9] lung,[10,11] and brain[12,13]) and their interactions *in vitro*.[3,14,15] Particularly, there emerged many biomimetic liver-on-a-chip (LOC) platforms. For example, Rennert *et al.* developed a liver organoid by integrating non-parenchymal cells (NPCs) and hepatocytes (HCs) into a suspended membrane.[16] Ma *et al.* developed a 3D-LOC platform of a liver-on-chip system based on cell spheroid culture and proposed the concept of long-term perfusion culture of three-dimensional human HepG2/C3A spheres for the establishment of three-dimensional liver spheroid

models. Ma *et al.* introduced a microporous membrane to simulate the physical barrier effect of fenestrated endothelial cells in the liver sinusoid to avoid the direct impact of high fluid shear stress on the hepatocytes, while maintaining high mass transfer perfusion conditions.[17] Long *et al.* developed a liver sinusoid platform by co-culturing of four types of rat primary hepatic cells by utilizing porous membranes.[18] These studies used porous membranes to support the cell growth that, in fact, is non-existent *in vivo*. Several studies presented scaffold-free liver chips.[19,20] Toh's group developed a microfluidic 3D hepatox chip (3D HepaTox chip), based on multiplexed microfluidic channels, to design a three-dimensional microenvironment in each channel to maintain the synthesis and metabolism of liver cells. They use micro-palisade arrays to support cell positioning and culture.[21] However, they fall short of fewer cell types or spatial arrangements varied from those *in vivo*.

In this study, we first used the liver chip technology in the field of hepatoprotective effect assessment. We first developed a new liver chip platform by exploiting the laminar flow and micro-fences in a microchannel. Specifically, we placed four types of hepatic cells (HepG2, HUVEC, LX-2, and U937 cells) into three fluidic layers, respectively, to reconstruct the structure of a liver sinusoid. Then, we perfused the culture medium though the artificial sinusoid by a gravity-driven flow, followed by application of this chip in the assessment of three hepatoprotective agents (tiopronin, bifendatatum, and glycyrrhizinate). We found that this chip not only can investigate the hepatoprotective effect but also can provide insights into the hepatoprotective mechanism, which can guide the following molecular biological studies.

## MATERIALS AND METHODS

### Fabrication of microfluidic device

The PDMS-glass composite microdevice was composed of two parts: a PDMS layer engraved with flow channels and culture chambers and a coverslip. The PDMS (Sylgard 184, Dow Corning, Midland, MI, USA) layer was replicated by an SU-8 (MicroChem, Westborough, MA, USA) mold, made according to standard soft lithography. Briefly, the SU-8 mold was 100 $\mu$m in height. PDMS prepolymer and cross-linker were mixed at the ratio of 10:1 (w/w) and poured onto the SU-8 template. After curing for 2 h at 80 °C, the PDMS layer was peeled from the mold, punched, and bonded to a coverslip by plasma oxidation.

### Cell culture

The medium for HepG2 culture (ATCC® HB-8065TM) is composed of 90% DMEM/high glucose medium (1×) containing 10% fetal bovine serum (Gibco™), 1% non-essential amino acids (NEAA) (Gibco™), 100 U ml$^{-1}$ penicillin, and 100 U ml$^{-1}$ streptomycin. The medium for HUVEC, LX-2, and U937 culture comprises 90% DME/F-12 1:1 (1×) medium, 10% fetal bovine serum (Gibco™), 100 U ml$^{-1}$ penicillin, and 100 U ml$^{-1}$ streptomycin. All cells were cultured in a cell incubator with 5% $CO_2$ at 37 °C.

### Manipulation of the cells in the microfluidic device

HepG2, HUVEC, and LX-2 cells were digested with trypsinase and made into cell suspension with $10^6$ cells/ml concentrations. Then, the cell suspensions were mixed with a 12 mg/ml ice-cold basement membrane extractant (BME) (R&D Systems, McKinley Place, MN, USA) separately at 1:1 ratio and loaded into a 1 ml syringe. The cell/BME mixtures were simultaneously injected into the microchannel (precooling treatment for avoiding premature mixture coagulation) using a multi-channel syringe pump (LSP10-1B, LongerPump®, China) through inlet 1 (HUVEC), inlet 2 (LX-2), and inlet 3 (HepG2) at a rate of 0.5 $\mu$l min$^{-1}$. After incubation for 30 min (37 °C, 5% $CO_2$) until BME was solidified, U937 cells, which were pre-exposed to 50 ng ml$^{-1}$ PMA (phorbol 12-myristate 13-acetate, Sigma-Aldrich) for 48 h,[22] were injected to the right perfusion channel and incubated for 2 h for attachment. Finally, a 200-$\mu$L pipet tip containing 100-$\mu$l "artificial blood" [DMEM-HG (Hyclone) medium supplemented with 10% fetal bovine serum (Gibco), 1% non-essential amino acids (Gibco), 100 U ml$^{-1}$ of penicillin, and 100 U ml$^{-1}$ of streptomycin] was inserted into the right perfusion inlet and an empty 200-$\mu$l pipet tip was placed at the corresponding outlet. Meanwhile, a 200-$\mu$l pipet tip containing 100-$\mu$l "artificial bile" ("artificial blood" without fetal bovine serum) was inserted into the left perfusion inlet and an empty 200-$\mu$l pipet tip was placed at the corresponding outlet. "Artificial blood" and "artificial bile" were replaced every 4 h.

### Cell viability assay

Live/death staining was conducted with the Calcein-AM-PI kit (KeyGEN BioTECH, Nanjing, China) according to the protocol. The viability of the cells was analyzed by MTT assay. Generally, the cells were trypsinized for 2 min and then rinsed out by the medium. Finally, the absorbance at 490 nm was measured with a microplate reader (H1MF9, Gene-tech, USA).

### Detection of urea and albumin

"Artificial blood" was collected from the perfusion channel every day and stored in a freezer in −80 °C before detection. The amounts of urea and albumin secreted into the perfusion channel were measured using a urea detection kit (C013-2, Nanjing Jiancheng Bioengineering Institute, China) and an albumin detection kit (A028-2, Nanjing Jiancheng Bioengineering Institute, China) according to the manuals.

### Testing of the activity of cytochrome P450 (CYP) 1A2 enzyme

CYP-1A2 activity was assessed by measuring O-dealkylation of the substrate 7-ethoxyresorufin (7-ER), according to a previous work.[7]

### Testing of acetaminophen (APAP) induced dose- and time-dependent hepatotoxicity

Acetaminophen (APAP) induced dose- and time-dependent hepatotoxicity was tested by measuring the amount of lactate dehydrogenase (LDH) released into the artificial blood. The LDH

content was determined using the CytoTox 96® Non-Radioactive Cytotoxicity Assay Kit (G1760, Promega, USA), according to the instruction.

### Measurement of LDH, aspartate transaminase (AST), and alanine transaminase (ALT) in the presence of hepatoprotectants

The chips were first perfused with a blank cell culture medium, tiopronin (100 $\mu$M, 1 mM, 2 mM, and 10 mM), bifendatatum (1 $\mu$M, 10 $\mu$M, 100 $\mu$M, and 1 mM), and glycyrrhizinate (1 $\mu$M, 10 $\mu$M, 100 $\mu$M, and 1 mM) for 24 h, respectively. Then, 2-mM APAP was loaded into chip with the "artificial blood" and incubated for another 24 h, followed by the collection of "artificial blood" for measurement. AST and ALT were measured according to the instruction of the AST and ALT detection assay kit (Nanjing Jiancheng Bioengineering Institute, China). The AST and ALT value based on the blank cell culture medium were used as control.

### Image processing and statistical analysis

Image processing was performed with ImageJ (National Institutes of Health, Bethesda, MD) software. The experimental results, including error bars in graphs, represent the mean ± standard deviation (SD). Student's $t$ test was used for statistical comparison. All experiments were repeated at least three times. Statistical significance was defined as $P \leq 0.05$.

## RESULTS

### Design and operation of the liver chip microdevice

Figure 1(a) shows the structure of the liver sinusoid, which is mainly composed of hepatocytes (HCs), hepatic stellate cells (HSCs), liver sinusoidal endothelial cells (LSECs), and Kupffer cells (KCs) in a specific spatial arrangement. HCs are the main functional cells and are locked to each other to form liver plates. LSECs are neatly arranged in a row to form a layer as a vessel wall. The gap between the two columns of cells is called perisinusoidal space where HSCs are located. KCs are located in the lumen of the hepatic blood vessels, just outside the LSECs layer. In general, the four types of cells are distributed in the liver as parallel bands with perfusion blood from the portal vein to the central vein providing permanent sustenance of nutrients and oxygen as well as removal of the waste metabolites.

Figure 1(b) shows the liver chip that simulates the liver sinusoid. The HCs, HSCs, and LSECs are deposited layer by layer inside the central microchannel under the regulation of the laminar flow

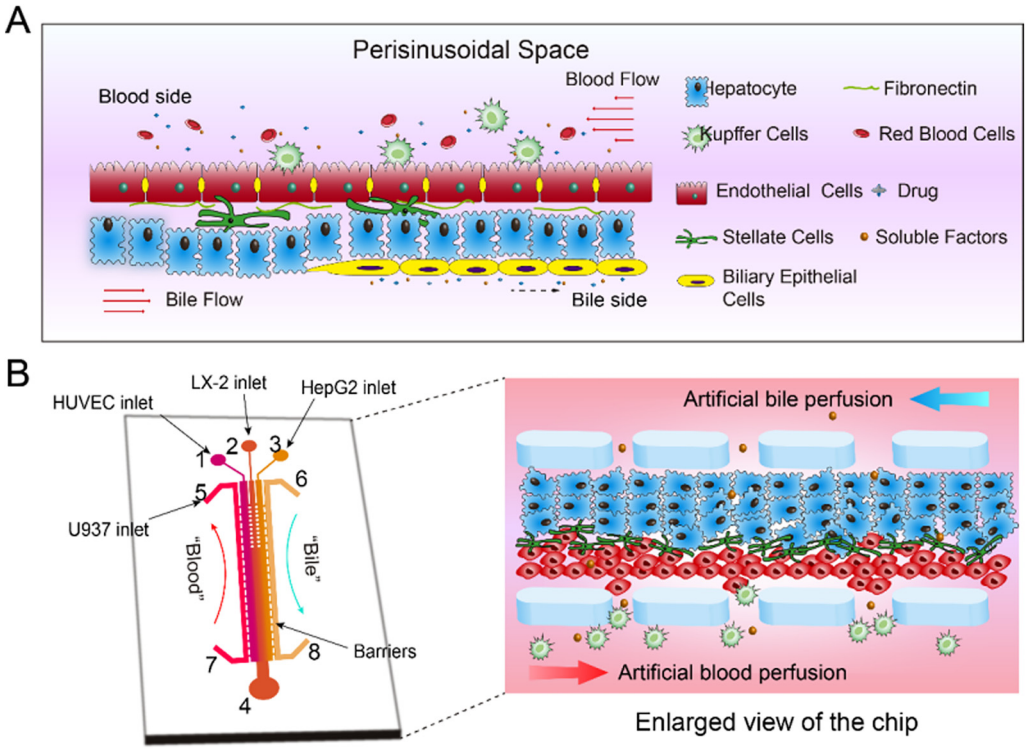


**FIG. 1.** Schematic diagram of the liver-on-a-chip design. (a) Microphysiological structure of hepatic sinusoids *in vivo* including cell composition, spatial arrangement, blood flow, and bile duct formation; (b) Schematic diagram of the liver-on-a-chip: (1) HUVEC cells inlet, (2) LX-2 cells inlet, (3) HepG2 cells inlet, (4) outlet, (5) and (7) artificial blood channel, and (6) and (8) artificial bile channel (enlarged for real cell arrangement in the chip). The central channel was 1 cm in length, 200 $\mu$m in width, and 100 $\mu$m in height. The side perfusion channels were 1 cm in length, 100 $\mu$m in width, and 100 $\mu$m in height. The gap between the micro-fences was 20 $\mu$m.

to form a sinusoid-like structure. The KCs are attached at the surface of LSECs layer. The microchannels for perfusion of artificial blood and bile are designed at the positions just beside the central microchannel, and the flow direction of artificial blood is opposite to that of the bile flow.

Figure 2 shows the straightforward operation of the liver chip. HUVECs, LX-2, and HepG2 cells were mixed with the BME gel, respectively, and then flowed into the central channel in parallel at the same speed of 0.5 $\mu$l/min, driven by a multi-channel syringe pump. After the incubation for 2 h, U937 cells were injected into the right perfusion channels for artificial blood flow. Next, four pipet tips (one for "blood," one for "bile," and two empty) were inserted into the outlets and inlets of the two perfusion channels. After a certain time, the artificial blood and bile were sampled for detection.

## Biological identification of the hepatic cell lines inside the liver chip

To avoid tedious operation of the primary hepatic cells from extraction to culturing, four types of immortal cell lines (HepG2, HUVEC, LX-2, and U937 cells) were used in this study. We first observed the morphology and biomarkers of the cell lines in conventional dishes for ensuring their functions. It was found that the HepG2 cells tended to connect with each other, which was similar to the aggregated HCs *in vivo*. Additionally, they expressed the albumin well [Fig. 3(a)]; HUVECs formatted tight junctions well and showed CD146 expression [Fig. 3(b)]; LX-2 expressed protein GFAP [Fig. 3(c)] and U937 expressed CD68 protein [Fig. 3(d)]. The distribution of these hepatic cells in the liver chip is shown in Figs. 3(e) and 3(f).

## Characterization of the function of the hepatic cells

We compared the cell viability in the liver chip platform to that in the traditional 96-well-plate model in 15 days [Fig. 4(a)]. It is shown in Fig. 4(b) that the cell viability in the chip was above 70%, while that in the well-plate model was <57% at the day 15. We also measured the liver-specific functions such as the albumin synthesis, urea secretion, and CYP-1A2 enzyme activity. As can be seen from Figs. 4(c) and 4(d), both albumin synthesis and urea secretion were higher in the liver chip than those in the

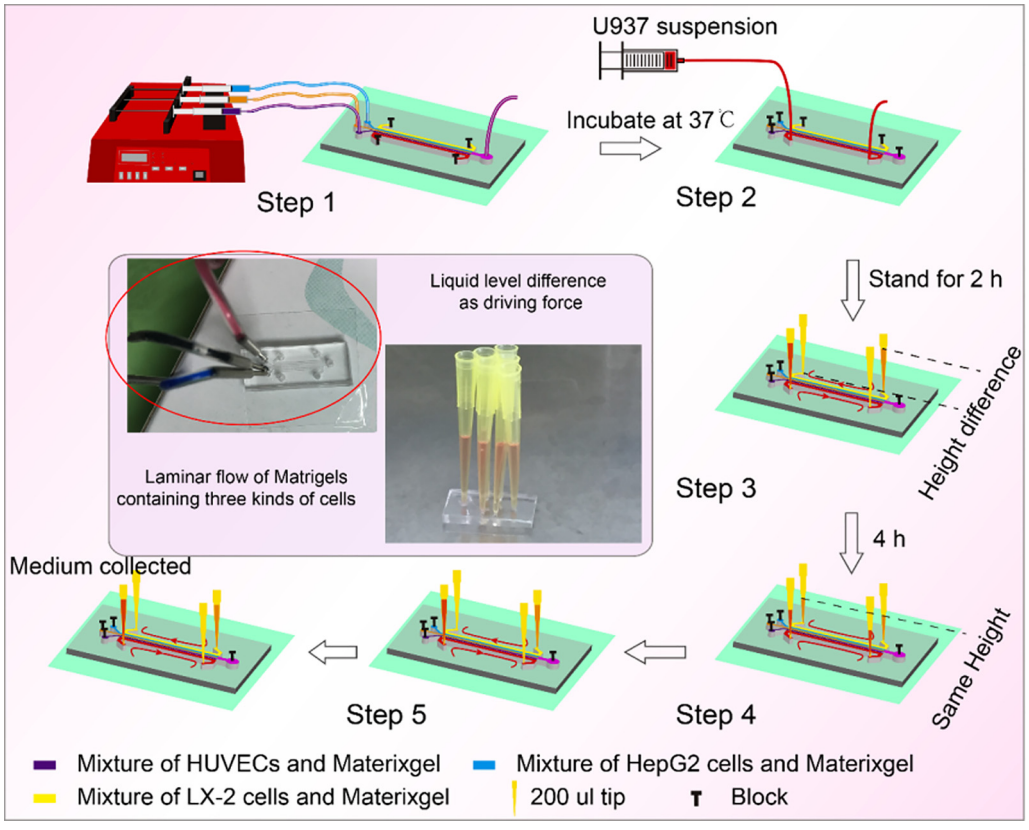


**FIG. 2.** Operation of the liver-on-a-chip. Step 1: Deposition of HUVEC, LX-2, and HepG2 cells simultaneously in the central microchannel by laminar flow; Step 2: Perfusion of U937 cells through the "artificial blood" channel. Step 3: Incubation for 2 h for attachment of U937 cells. Step 4: Loading of hepatoprotectants. Step 5: Loading of APAP.

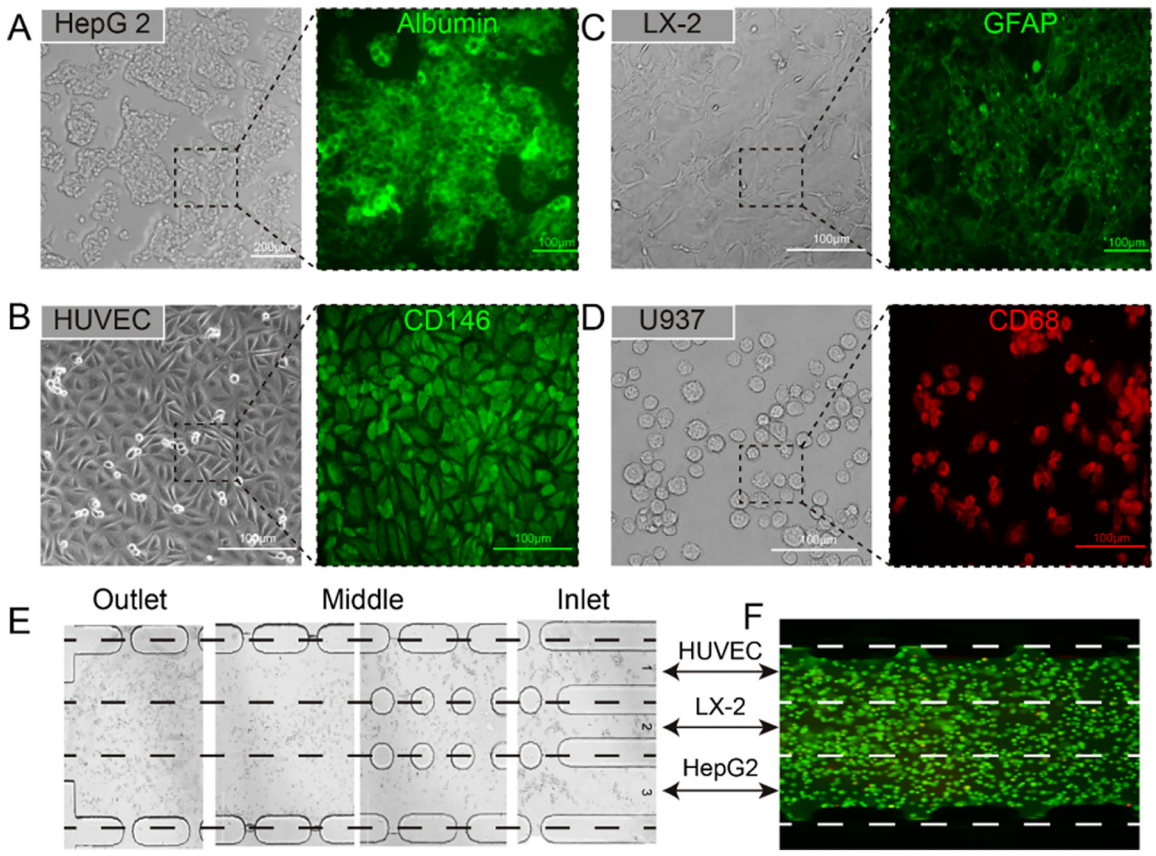


**FIG. 3.** Characterization of four types of hepatic tumor cell lines in a Petri dish (a)–(d), including bright field images of HepG2, HUVEC, LX-2, and U937 cells after culturing for two days and key proteins expressions, such as albumin (HepG2 cells), CD146 (HUVEC cells), GFAP (LX-2 cells), and CD68 (U937 cells). (e) and (f), Cell deposition in central microchannel by the laminar flow. The green fluorescence in (f) was generated by Calcein-AM.

96-well-plate. Particularly, at the later stage, they dropped sharply in the 96-well-plate while was maintained at a high level in the liver chip. This phenomenon may be attributed to the biomimetic 3D microenvironments in the liver chip, which enhanced the phenotypes of the hepatic cells. We further investigated the activity of CYP 1A/2 enzymes and found that the CYP 1A/2 activity in the liver chip [Fig. 4(e)] was higher than in 96-well-plate at day 8 and day 15. All these results demonstrated the superiority of the liver chip over the traditional 96-well-plate model.

## Dose- and time-dependent hepatotoxicity induced by APAP

In this study, APAP, a commonly used analgesic worldwide, was introduced into the liver chip to develop a drug-induced acute liver injury model. Artificial blood was spiked with different concentrations of APAP (1 $\mu$M, 10 $\mu$M, 100 $\mu$M, 1 mM, 5 mM, 10 mM, and 20 mM) at day 3. Live/dead staining was operated after another 24 h. The results were shown in Fig. 5(a), showing that when the concentration was lower than 100 $\mu$M, there was no significant change in cell viability; while the concentration continued to increase, the cell activity decreased sharply. According to these results, we plotted the dose-dependent hepatotoxicity profile [Fig. 5(b)] with $R^2 = 0.997$ with MTT assays. Also, we tested the time-dependence of APAP hepatotoxicity at the concentration of 10 mM. It showed that the toxicity of APAP showed a significant temporal dependence and entered a plateau after 24 h.

## Evaluating the hepatoprotective effect of tiopronin, bifendatatum, and glycyrrhizinate

According to the dose- and time-dependent hepatotoxicity induced by APAP (Fig. 5), 20-mM APAP and 24 h of exposure time were chosen to create the model of drug-induced liver disease. We tested the effect of three known hepatoprotectants (tiopronin, bifendatatum, and glycyrrhizinate) with LDH, ALT, and AST as indicators. It can be seen that all these three drugs had the significant ability to reduce LDH, ALT, and AST levels (Fig. 6); however, their ability to reduce each indicator varied from each other. As

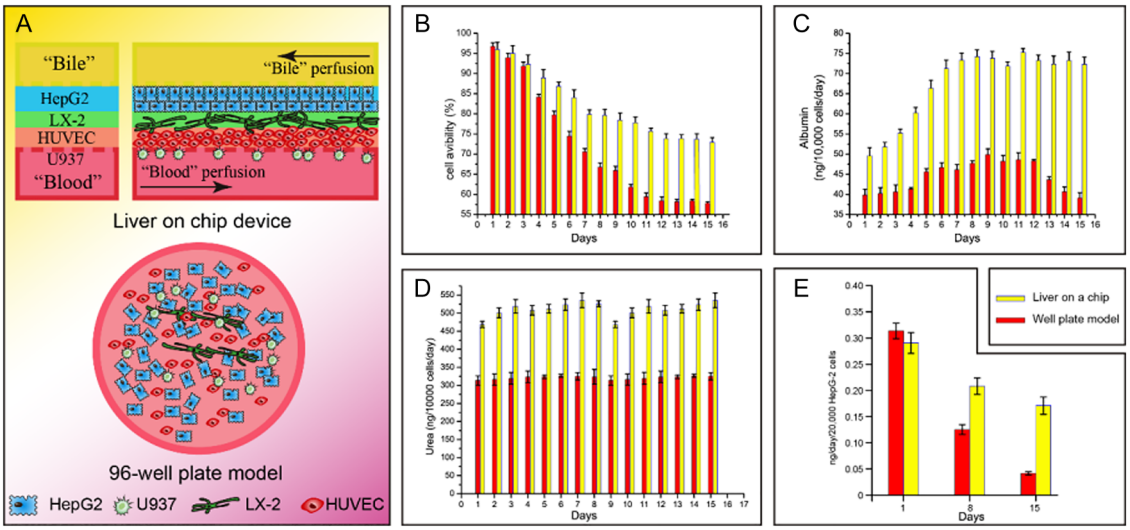


**FIG. 4.** Comparison of the liver chip device with the traditional 96-well-plate model. (a) Illustration of the liver chip and 96-well-plate model. (b) Cell viability within 15 days. (c) and (d) Urea production and albumin synthesis within 15 days. (e) Enzymatic activity of CYP-1A2.

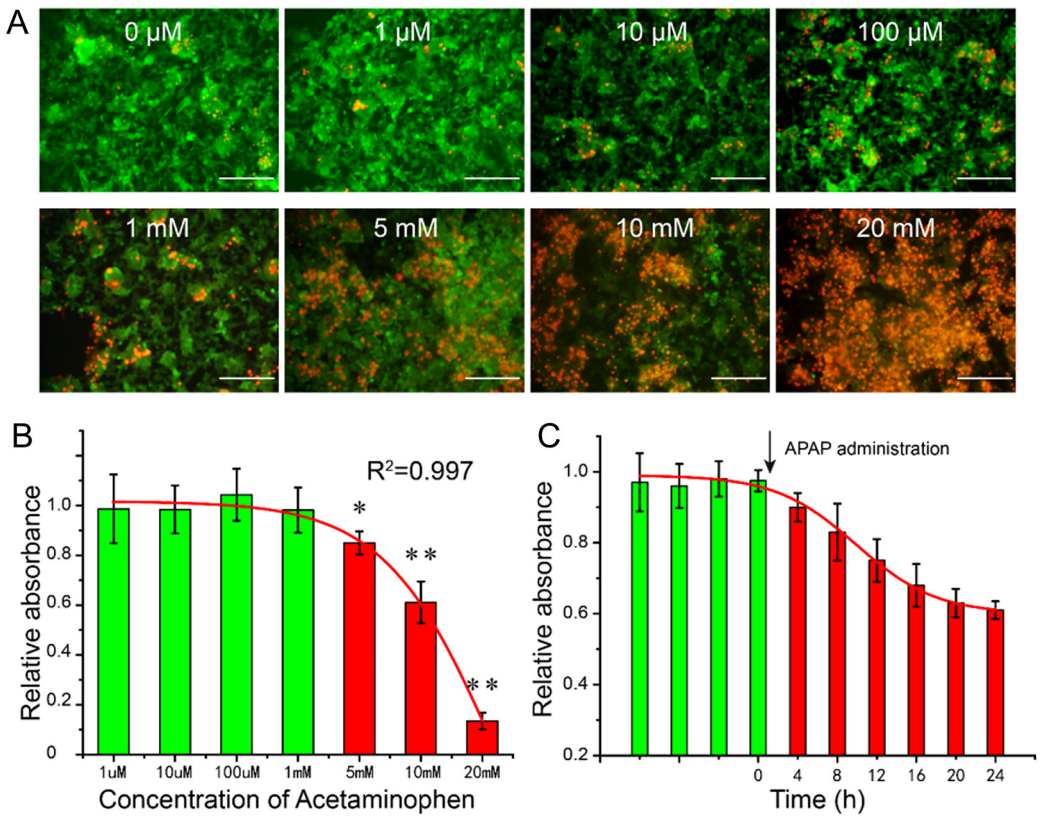


**FIG. 5.** Dose- and time-dependent hepatotoxicity of APAP. (a) Representative images of the cells in the central channel stimulated by different concentrations of APAP with live/death staining. Scale bar = 200 $\mu$m. (b) Dose-dependent hepatotoxicity of APAP on day 3. (c) Time-dependent hepatotoxicity of APAP at the concentration of 10 mM.

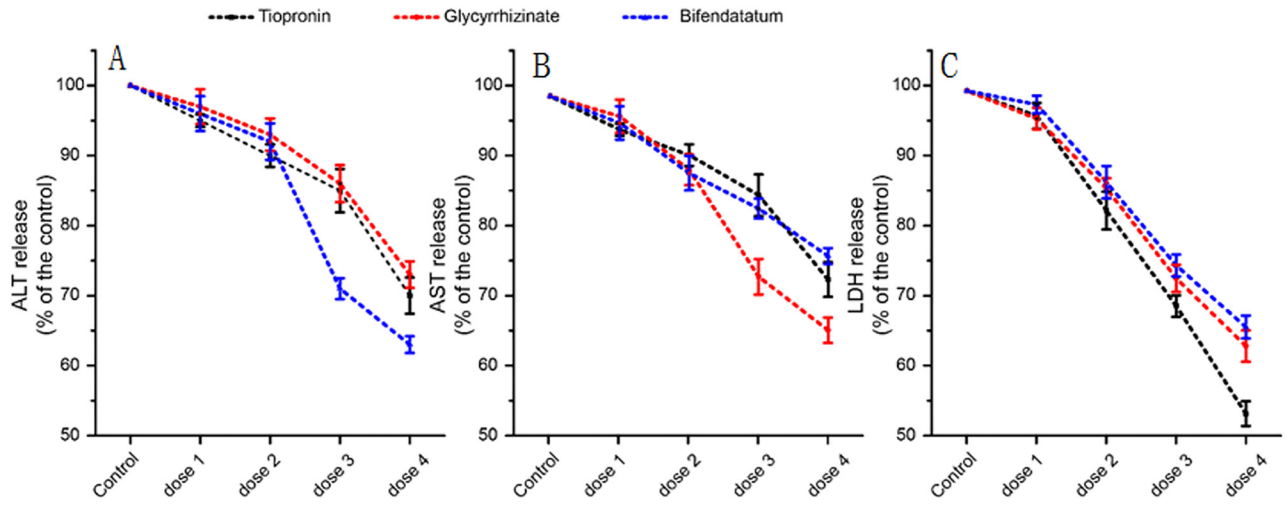


**FIG. 6.** Evaluating liver-protecting effect of tiopronin, bifendatatum, and glycyrrhizinate through three liver disease indicators (ALT, AST, and LDH release). Dose 1, 2, 3, and 4 referred to the experimental section. (a) ALT release after treated with hepatoprotectants, (b) AST release after treated with hepatoprotectants, and (c) LDH release after treated with hepatoprotectants.

shown in Fig. 6(a), 1-mM bifendatatum decreased ALT by 37%, while 10-mM tiopronin and 1-mM glycyrrhizinate decreased by 30% and 26%, respectively. As shown in Fig. 6(b), 1-mM glycyrrhizinate decreased AST by 35%, while 10-mM tiopronin and 1-mM bifendatatum decreased by 27.5% and 24.5%, respectively. As shown in Fig. 6(c), 10-mM tiopronin decreased ALT by 46.5%, while 1-mM glycyrrhizinate and 1-mM bifendatatum decreased by 37.5% and 34.5%, respectively.

## DISCUSSION

Liver disease is one of the major concerns of human health globally, which is related to a lot of factors including viruses, bacteria, parasitic infections, improper diet, alcohol, and other diseases.[23] The main means of treatment of liver disease is to eliminate the cause followed with nutritional support. As a support strategy, applying hepatoprotectants can quickly improve the disease status and accelerate the improvement of the disease. Currently, various liver-protecting drugs are sold on the market with different mechanisms. Traditionally, well-plate models are widely used for a pre-clinical study of hepatoprotective effect and mechanism; however, these models are not perfect because of lacking *in vivo* similar microenvironments such as 3D culture condition and perfusion.

In this study, a quick screening device for hepatoprotective drugs was proposed. Its advantages can be summarized as follows: (1) Four types of hepatic cell line could simultaneous inoculate into the cell chamber according to laminar flow. This method is easy to operate and time saving, because it only needs a multichannel low speed syringe pump. (2) Gravity-induced potential difference of liquid was applied for perfusion to simulate liver sinusoid blood flow and bile efflux, which simplifies the instrumentation. (3) There is no need for any separators, such as porous PC membrane, for supporting spatial arrangement of different types of cells. (4) Low reagent consumption due to the whole volume of the channel is only 0.5 $\mu$l, which is much smaller than a 96-well-plate.

Moreover, the liver chip is also superior to the traditional model in terms of bionics. The culture period and liver-specific functions are the basic parameters of the *in vitro* liver model. Our results showed [Fig. 4(b)] that compared to the traditional well-plate model, this device's cell viability could still maintain above 70% at day 15. The excretion of both urea and albumin [Figs. 4(c) and 4(d)] was higher in the liver chip, reaching 532.5 and 72.5 ng/day/10 000 cells at day 15, respectively. Furthermore, CYP-1A2 activity [Fig. 4(e)] is much higher than the well-plate model during this period. All these mean that this device is superior to the traditional well-plate model, which could own the device's specific structure that allows a more bio-mimic microenvironment.

The highlight of this device is its ability to reflect the dose- and time-dependent hepatotoxicity of APAP and evaluate the effectiveness of hepatoprotectants. In this study, APAP-induced liver injury was used as a disease model for evaluation of hepatoprotectants, not only because it is a classical drug-induced injury case but also owing to its easy reversal after medical treatment.[24] Using this device, we tested APAP's hepatotoxicity on day 3, as shown in Fig. 5(a). As the concentration of APAP increases, the hepatotoxicity was gradually increased. When the concentration reached 20 mM, the survival rate was less than 20%. Furthermore, we tested the time-dependent hepatotoxicity of APAP. Cell viability decreased sharply in the first 24 h after dosing and then remained at a stable level. Thus, the dose- and time-dependent APAP-induced disease model was constructed. Using

APAP-induced liver disease, we tested the effect of liver protection of three commercially available liver protection drugs (tiopronin, bifendatatum, and glycyrrhizinate). We found that all three drugs exhibited a liver-protecting effect at low concentrations, while their ability to reduce each liver injury indicators varied (Fig. 6). We summarized these results: in reducing ALT release, bifendatatum > tiopronin > glycyrrhizinate; in reducing AST release, glycyrrhizinate > tiopronin > bifendatatum; in reducing LDH release, tiopronin > glycyrrhizinate > bifendatatum. These results suggest that specific medical treatment should be applied for different liver injury symptoms, instead of trying drugs one by one. This study provides a basis for guidance on clinical liver disease medication. However, this is just a start. More trials could be conducted to determine which drug suits liver disease symptoms, which will save lots of time and money.

## CONCLUSION

In conclusion, this paper presented a new method to fabricate a liver sinusoid chip. It uses micro-fences and laminar flow in a microchannel to distribute the four types of hepatic cells layer by layer in the microchannel. This method is free of porous membrane, which facilitates *in situ* fluorescence imaging. This liver chip demonstrated high cellular activity and active expression of biochemical indicators (albumin, urea) and drug-metabolizing enzymes compared with the traditional 96-well-plate model. This liver chip enabled measurement of the dose- and time-dependent hepatotoxicity of acetaminophen. This liver chip also enabled investigation of the hepatoprotective effect and mechanism of candidate hepatoprotectants, which paved the way for the next-step molecular biological study.

## SUPPLEMENTARY MATERIAL

See the supplementary material for the photograph of the liver-on-a-chip device.

## AUTHORS' CONTRIBUTIONS

J. Deng, Y. Luo, and X. Zhang designed the study; J. Deng performed the experiments; J. Deng, Y. Cong, X. Han, W. Wei, and Y. Luo analyzed the data and discussed the experiments; J. Deng, Y. Cong, X. Han, Y. Luo, Y. Lu, and T. Liu wrote the paper. W. Zhao and B. Lin supervised the whole project. All authors approved the final manuscript. J. Deng, Y. Cong, and X. Han contributed equally to this work.

## ACKNOWLEDGMENTS

This work was supported by the National Natural Science Foundation of China (No. 21675017) and the National Key Research and Development Program of China (No. 2017YFC1702001).

The authors declare neither conflict of interest nor competing financial interest.

## DATA AVAILABILITY

The data that support the findings of this study are available within the article and its supplementary material.

## REFERENCES

[1]M. Pinzani and K. Rombouts, "Liver fibrosis: From the bench to clinical targets," Dig. Liver Dis. **36**(4), 231–242 (2004).
[2]P. Godoy, N. J. Hewitt, U. Albrecht *et al.*, "Recent advances in 2D and 3D in vitro systems using primary hepatocytes, alternative hepatocyte sources and non-parenchymal liver cells and their use in investigating mechanisms of hepatotoxicity, cell signaling and ADME," Arch. Toxicol. **87**(8), 1315–1530 (2013).
[3]J. H. Sung, Y. I. Wang, N. Narasimhan Sriram *et al.*, "Recent advances in body-on-a-chip systems," Anal. Chem. **91**(1), 330–351 (2018).
[4]V. M. Lauschke, D. F. G. Hendriks, C. C. Bell *et al.*, "Novel 3D culture systems for studies of human liver function and assessments of the hepatotoxicity of drugs and drug candidates," Chem. Res. Toxicol. **29**(12), 1936–1955 (2016).
[5]B. R. Ware and S. R. Khetani, "Engineered liver platforms for different phases of drug development," Trends Biotechnol. **35**(2), 172–183 (2016).
[6]J. Deng, X. Zhang, Z. Chen *et al.*, "A cell lines derived microfluidic liver model for investigation of hepatotoxicity induced by drug-drug interaction," Biomicrofluidics **13**(2), 24101 (2019).
[7]J. Deng, W. Wei, Z. Chen *et al.*, "Engineered liver-on-a-chip platform to mimic liver functions and its biomedical applications: A review," Micromachines **10**(10), 676 (2019).
[8]A. Petrosyan, P. Cravedi, V. Villani *et al.*, "A glomerulus-on-a-chip to recapitulate the human glomerular filtration barrier," Nat. Commun. **10**(1), 3656 (2019).
[9]S. G. Rayner, K. T. Phong, J. Xue *et al.*, "Reconstructing the human renal vascular-tubular unit in vitro," Adv. Healthcare Mater. **7**(23), 1801120 (2018).
[10]K. H. Benam, R. Villenave, C. Lucchesi, *et al.*, "Small airway-on-a-chip enables analysis of human lung inflammation and drug responses in vitro," Nat. Methods **13**(2), 151–157 (2016).
[11]X. Yang, K. Li, X. Zhang *et al.*, "Nanofiber membrane supported lung-on-a-chip microdevice for anti-cancer drug testing," Lab Chip **10**, 1039 (2018).
[12]B. M. Maoz, A. Herland, E. A. Fitzgerald *et al.*, "A linked organ-on-chip model of the human neurovascular unit reveals the metabolic coupling of endothelial and neuronal cells," Nat. Biotechnol. **36**(9), 865–874 (2018).
[13]E. Karzbrun, A. Kshirsagar, S. R. Cohen *et al.*, "Human brain organoids on a chip reveal the physics of folding," Nat. Phys. **14**(5), 515–522 (2018).
[14]Y. S. Zhang, J. Aleman, S. R. Shin *et al.*, "Multisensor-integrated organs-on-chips platform for automated and continual in situ monitoring of organoid behaviors," Proc. Natl. Acad. Sci. U.S.A. **114**(12), E2293–E2302 (2017).
[15]A. Guan, P. Hamilton, Y. Wang *et al.*, "Medical devices on chips," Nat. Biomed. Eng. **1**(3), 45 (2017).
[16]K. Rennert, S. Steinborn, M. Gröger *et al.*, "A microfluidically perfused three dimensional human liver model," Biomaterials **71**, 119–131 (2015).
[17]L.-D. Ma, Y.-T. Wang, J.-R. Wang *et al.*, "Design and fabrication of a liver-on-a-chip platform for convenient, highly efficient, and safe in situ perfusion culture of 3D hepatic spheroids," Lab Chip **17**(18), 2547–2562 (2018).
[18]Y. Du, N. Li, H. Yang *et al.*, "Mimicking liver sinusoidal structures and functions using a 3D-configured microfluidic chip," Lab Chip **17**(5), 782–794 (2017).
[19]Y. Weng, S. Chang, M. Shih *et al.*, "Scaffold-free liver-on-a-chip with multiscale organotypic cultures," Adv. Mater. **29**(36), 1701545 (2017).
[20]S. Mi, X. Yi, Z. Du *et al.*, "Construction of a liver sinusoid based on the laminar flow on chip and self-assembly of endothelial cells," Biofabrication **10**(2), 25010 (2018).
[21]Y. Toh, T. Lim, D. Tai *et al.*, "A microfluidic 3D hepatocyte chip for drug toxicity testing," Lab Chip **14**(9), 2026 (2009).
[22]L. Prodanov, R. Jindal, S. S. Bale *et al.*, "Long-term maintenance of a microfluidic 3D human liver sinusoid," Biotechnol. Bioeng. **113**(1), 241–246 (2016).
[23]A. Rocco, "Alcoholic disease: Liver and beyond," World J. Gastroenterol. **20**(40), 14652 (2014).
[24]C. Li, Y. Ming, Z. Wang *et al.*, "GADD45α alleviates acetaminophen-induced hepatotoxicity by promoting AMPK activation," Cell. Mol. Life Sci. **76**(1), 129–145 (2019).